THE ASTROPHYSICAL JOURNAL, 426:801–811, 1994 May 10

MEASURING THE HELIUM ABUNDANCE IN THE SOLAR ENVELOPE: THE ROLE OF THE EQUATION OF STATE

H. M. ANTIA[1] AND SARBANI BASU
Tata Institute of Fundamental Research, Homi Bhabha Road, Bombay 400 005, India
Received 1993 August 23; accepted 1993 November 16

ABSTRACT

Variations in the adiabatic index of stellar material in the second helium ionization zone enable one to infer the helium abundance in the solar envelope, using the observed frequencies of solar oscillations. Three techniques based on the differential asymptotic method for sound speed inversion are considered. With the help of the signature of helium abundance on various tracers of ionization, it is possible to estimate the helium abundance. Using several test models, the systematic errors in these techniques are estimated. All these techniques are found to be sensitive to the equation of state. The MHD equation of state is found to be close to that of solar material. Using reference models employing MHD equation of state we find the solar helium abundance $Y = 0.252 \pm 0.003$.

Subject headings: Sun: abundances — Sun: interior — Sun: oscillations

1. INTRODUCTION

Direct seismological measurements of the helium abundance in the solar convection zone can be obtained from a variation of the adiabatic index of the stellar material in the ionization zones. The second helium ionization zone is particularly well suited for this purpose because it occurs sufficiently deep in the convection zone where the stratification is essentially adiabatic and as a result the temperature gradient is independent of the opacity of the stellar material. Further, at this depth the Reynold stresses are not expected to be important. The variation in the adiabatic index depends predominantly on the relative abundances, X and Y, of hydrogen and helium, although there might be some contribution from the heavier elements, some of which will also be undergoing ionization in the same region. The lowering of the adiabatic index in the ionization region will affect the sound speed profile, but the sound speed itself varies too rapidly with depth to reveal the modulation. However, as Gough (1984) has pointed out, we can use the radial gradient of sound speed to study the modulation in the adiabatic index. For adiabatic stratification (cf. Gough 1984),

$$W = \frac{r^2}{Gm}\frac{dc^2}{dr} = \frac{1-\gamma_\rho-\gamma}{1-\gamma_{c^2}}, \qquad (1)$$

where $\gamma = (\partial \ln p/\partial \ln \rho)_S$, $\gamma_\rho = (\partial \ln \gamma/\partial \ln \rho)_{c^2}$, $\gamma_{c^2} = (\partial \ln \gamma/\partial \ln c^2)_\rho$, m is the mass in the spherical shell of radius r, and G is the gravitational constant. Below the helium ionization zone where the stellar material is almost fully ionized, $W \approx -\frac{2}{3}$. Using the sound speed profile of a solar model, Däppen & Gough (1986) plotted W as a function of radius to show two distinct humps close to the solar surface. The smaller hump at $r \approx 0.98\ R_\odot$ corresponds to the He II ionization zone, while the bigger hump at $r > 0.99\ R_\odot$ corresponds to the ionization of H I and He I. Although H I and He I ionizations give rise to a much bigger hump, it is difficult to use them for helioseismic purposes, because the stratification in the immediate subsurface layers departs considerably from the adiabatic, and there are significant uncertainties in the temperature gradient in this region arising from lack of any reliable treatment of convection.

Using the sound speed profiles of several solar models, Däppen & Gough (1986) found that the height of the He II hump essentially depends on Y, while the position of the hump depends on the mixing-length parameter α. Thus using the information on position and height of the hump it is possible to determine α and Y for a solar model. This technique can be employed to estimate the helium abundance in the Sun by using the sound speed profile obtained from inversion of helioseismic data. However, it was found that errors introduced during the differentiation of the inverted sound speed profile using asymptotic inversion did not allow an unambiguous identification of the He II hump. Däppen, Gough, & Thompson (1988a) used a differential technique to obtain the sound speed for a solar model and demonstrated the feasibility of this technique for determining the helium abundance. Nevertheless, they concluded that the observed frequencies were not sufficiently accurate to determine the helium abundance reliably.

Vorontsov, Baturin, & Pamyatnykh (1992) calibrated the asymptotic phases of solar oscillations against those of a sequence of theoretical models to obtain $Y = 0.25 \pm 0.01$. They also found that the results are fairly sensitive to the equation of state. Similarly, Christensen-Dalsgaard & Pérez Hernández (1991) used scaled frequency differences between the frequencies for a solar model and observed frequencies and found $Y \approx 0.25$. On the other hand, using a nonasymptotic inversion technique, Däppen et al. (1991) found $Y = 0.268 \pm 0.01$. With a similar technique, Dziembowski, Pamyatnyky, & Sienkiewicz (1991) obtained $Y = 0.234 \pm 0.005$. Kosovichev et al. (1992) studied the uncertainties involved in the nonasymptotic techniques for determining the helium abundance and concluded that the main source of uncertainty is the equation of state. By comparing the observed frequencies with those obtained for solar models which include diffusive settling of helium and metals, Guzik & Cox (1993) found $Y = 0.24 \pm 0.005$ in the solar envelope.

It is clear that the helioseismic measurement of helium abundance is sensitive to the equation of state of stellar material. By comparing the asymptotic phases of oscillations calculated for a solar model with those calculated from the observed fre-

[1] E-mail: antia@tifrvax.bitnet

quencies, Vorontsov et al. (1992) concluded that the MHD equation of state (Hummer & Mihalas 1988; Mihalas, Däppen, & Hummer 1988; Däppen et al. 1988b) gives results which are very close to observations. Christensen-Dalsgaard, Däppen, & Lebreton (1988) also found that the MHD equation of state yields frequencies that are closer to observations. It is difficult to estimate the systematic errors in the helium abundance measurements because of uncertainties in the equation of state, but the effect of uncertainty in the equation of state is not the same in all techniques for measuring helium abundance. Thus, by comparing results obtained using independent techniques it may be possible to estimate uncertainties in measured values of Y.

In the present work we use three different techiques for measuring Y using solar oscillations frequencies. One of the techniques is similar to that of Däppen et al. (1988a) where we estimate the height of He II hump in the function W defined by equation (1) using the sound speed obtained by the differential asymptotic inversion (Christensen-Dalsgaard, Gough, & Thompson 1989) of oscillation frequencies. The differential technique gives a relatively smooth profile for c^2, and it is thus possible to identify the He II hump in the computed values of W. However, the height of the hump does depend to some extent on the underlying reference model. The other methods used in this work are also based on the differential asymptotic inversion, but instead of using the sound speed, we use the functions $H_1(w)$ and $H_2(\omega)$ [where $w = \omega/(l + 1/2)$] which isolate the contribution to the frequency changes due to the interior and surface layers, respectively. This technique is similar to that used by Christensen-Dalsgaard & Pérez Hernández (1991) except for the fact that they did not separate the frequency difference in terms of the two functions $H_1(w)$ and $H_2(\omega)$. In the absence of this separation the scaled frequency difference is likely to be dominated by uncertainties in surface layers which are difficult to isolate. It is known that the function $H_1(w)$ also has humps (or dips) corresponding to the ionization zones of hydrogen and helium. The function $H_2(\omega)$ which characterizes the contribution due to surface layers may be expected to be dominated by the differences in H I and He I ionization zones.

In each of these techniques, we calibrate the amplitude of the He II hump using a sequence of envelope models with different helium abundances. The calibration can also be affected by the mixing length parameter, α. However, we can eliminate α as it essentially determines the depth of the convection zone in a solar envelope model. Since the depth of the solar convection zone is now known fairly accurately (Christensen-Dalsgaard, Gough, & Thompson 1991), for each value of Y we fix the value of α by demanding that the depth of convection zone in the model to be 200,000 km. Thus only one free parameter enters the sequence of envelope models. In order to estimate the effect of a difference in the convection zone depth on determination of helium abundance, we have tried to estimate the helium abundance in models with different depths of convection zone using the same calibration models. To study the influence of equation of state, we use solar envelope models with different equations of state.

2. THE INVERSION METHOD

In order to measure the helium abundance we use the differential asymptotic method for sound speed inversion (Christensen-Dalsgaard et al. 1989). In this method, the frequency difference between a pair of solar models (or the difference between frequencies of a solar model and the observed solar frequencies) is used to find the corresponding sound speed difference between the models (or between a solar model and the Sun). One of the models serves as a reference model whose sound speed is already known to determine the sound speed profile in the second model (or the Sun). Since we are interested only in the helium ionization zones, it is not necessary to use a full solar model. Instead, we use solar envelope models extending to a depth of 250,000 km from the photosphere and consider only those modes which are trapped well within this depth.

For the purpose of calibration, we have constructed a sequence of solar envelope models with different helium abundances. The envelope models also depend on the mixing-length parameter α, but as explained earlier for a given value of Y, α is chosen to give the correct depth of convection zone. Thus our reference models are only a function of Y. In order to study the sensitivity of our technique to the equation of state, we have constructed solar envelope models using three different equations of state: (1) EFF equation of state (Eggleton, Faulkner, & Flannery 1973); (2) equation of state using the Planck-Larkin partition function (Ebeling, Kraeft, & Kemp 1976; Rogers 1977), where all Boltzmann factors of the form $e^{-E/kT}$ in the Saha equation are replaced by $e^{-E/kT} - 1 + (E/kT)$; and (3) the so-called MHD equation of state (Däppen et al. 1988b). Thus we have constructed a sequence of models EFF64, EFF66, EFF68, EFF70, EFF72, EFF74, and EFF76 with the hydrogen abundance varying between 64% and 76%, using the EFF equation of state and models PLPF64, PLPF66, PLPF68, PLPF70, PLPF72, PLPF74, and PLPF76 using the Planck-Larkin partition function. All these models have a metal abundance $Z = 0.018$, with relative abundance as given by Vernazza, Avrett, & Loeser (1973). Similarly, we have models MHD68, MHD70, MHD72, MHD74, and MHD76 with the hydrogen abundance varying between 68% and 76%, using the MHD equation of state. All the MHD models have metal abundance $Z = 0.02$ since that is the only value available in our MHD tables. Further all these reference models use the OPAL opacities (Rogers & Iglesias 1992). Any of these models can be used as a reference model in the differential asymptotic technique. In order to test our technique for determining the helium abundance, we have constructed test models using each of these equations of state. Some of these models have different convection zone depths. The properties of these test models are summarized in Table 1, where r_d is the radial distance of the base of the convection zone. All the test models except M6 use OPAL opacities, while model M6 is constructed using the opacity tables of Cox & Tabor (1976). Models M1, M4, and M7 are envelope models which have been constructed using a procedure similar to that for the reference models. All the EFF and PLPF models (except M4) use the solar abundance (cf.

TABLE 1

PROPERTIES OF TEST MODELS

Model	EOS	Opacity	$r_d/R_\odot$	X	Y	Z
M1.....	EFF	OPAL	0.7098	0.7300	0.2500	0.0200
M2.....	EFF	OPAL	0.7303	0.7198	0.2622	0.0180
M3.....	EFF	OPAL	0.7950	0.6675	0.3145	0.0180
M4.....	EFF	OPAL	0.7110	0.7200	0.2600	0.0200
M5.....	PLPF	OPAL	0.7124	0.7127	0.2693	0.0180
M6.....	PLPF	Cox-Tabor	0.7220	0.7438	0.2382	0.0180
M7.....	MHD	OPAL	0.7142	0.7100	0.2700	0.0200

Vernazza et al. 1973) for metals, while the MHD models use only C, N, O, and Fe with the abundance of Fe adjusted to make $Z = 0.02$. In order to study the influence of variation in metal abundance on the determination of Y, we have constructed the model M4 which is similar to the reference model EFF72 except for the fact that it has the same metal abundances as the MHD models. Models M2, M3, M5, and M6 are full solar models constructed using different equations of state or opacities. Models M5 and M6 employ a nonlocal mixing-length formulation (Antia, Chitre, & Narasimha 1984), while all other models, including the reference models, use a local mixing-length theory. The model M3 has been constructed using a homogeneous composition, where the helium abundance and the mixing-length parameter α were adjusted to get the correct radius and luminosity.

Following Christensen-Dalsgaard et al. (1989) we express the scaled frequency difference in the form

$$S(w)\frac{\omega_0 - \omega}{\omega_0} = H_1(w) + H_2(\omega)\,, \tag{2}$$

where

$$S(w) = \int_{r_t}^{R_\odot} \left(1 - \frac{c_0^2}{w^2 r^2}\right)^{-1/2} \frac{dr}{c_0}\,, \tag{3}$$

and

$$H_1(w) = \int_{r_t}^{R_\odot} \left(1 - \frac{a^2}{w^2}\right)^{-1/2} \frac{c_0 - c}{c_0}\frac{1}{a}\frac{dr}{r}\,. \tag{4}$$

Here $r_t = c_0/w$ is the lower turning point, c_0 is the sound speed in the reference model, and c is the sound speed in the test model or the Sun, $a = c_0/r$, ω_0 is the frequency of p-mode in the reference model, while ω is the frequency of the same mode in another solar model or the observed frequency. Hence the scaled frequency difference depends asymptotically on the interior sound speed difference through a function of w, and on differences in the surface layers through a function of ω. Using the known frequency difference between a large number of modes we can obtain the functions $H_1(w)$ and $H_2(\omega)$ by a least squares solution of equation (2). For this purpose we expand $H_1(w)$ in terms of B-spline basis functions in log w and similarly expand $H_2(\omega)$ using B-splines in ω. For both these functions we use 20 knots uniformly spaced in log w and ω, respectively. We have done experiments to find that the results are not sensitive to the number of knots used. Since in this work we are interested only in envelope models we consider only those modes for which $1.0 < \omega < 5.0$ mHz and $w < 0.1$ mHz. Further, since we wish to use this technique on observed frequencies also, we restrict the sample of modes to those listed in the tables of Libbrecht, Woodward, & Kaufman (1990) and weigh each point according to the quoted standard deviation in the frequencies. Since the asymptotic relation cannot be expected to hold for the f-mode, we also reject the f-mode ($n = 0$) from the set of modes to be used for inversion. After applying these cutoffs we are left with about 2070 eigenmodes to calculate $H_1(w)$ and $H_2(\omega)$. For obtaining the least-squares solution of equation (2) we use singular value decomposition (SVD) (cf. Antia 1991) which directly gives the coefficients of both sets of B-splines. It may be noted that the functions $H_1(w)$ and $H_2(\omega)$ cannot be determined uniquely; thus for example, for any set of solutions H_1 and H_2, $H_1 + b$ and $H_2 - b$ will also be a solution where b is any arbitrary constant. As explained later, this nonuniqueness does not cause any problem with the determination of helium abundance.

Using the function $H_1(w)$ determined as above, we can obtain the difference in sound speeds between the two models or between that in the Sun and the reference model using

$$\frac{c_0 - c}{c_0} = -\frac{2r}{\pi}\frac{da}{dr}\int_{a_s}^{a} \frac{(dH_1/dw)w\,dw}{(a^2 - w^2)^{1/2}}\,, \tag{5}$$

where $a_s = a(R_\odot)$. Equation (5) is slightly different from the corresponding equation in Christensen-Dalsgaard et al. (1989), but it can be easily shown that the two expressions are equivalent. Using the calculated sound speed c for the solar model (or the Sun), we can then easily compute the function $W(r)$ using equation (1).

3. HELIUM ABUNDANCE USING $H_1(w)$

For determining the helium abundance in the solar envelope it is not essential to compute the sound speed, since the functions $H_1(w)$ and $H_2(\omega)$ also exhibit the signature of the difference in Y between the two models. Figure 1 shows the functions $H_1(w)$ between the reference models EFF68, EFF70, EFF72, EFF74, EFF76 and the solar envelope model M1 (see Table 1). Each of the curves shows two humps, one at $\log w \approx -2$ mHz and the other at $\log w \approx -2.25$ mHz. The first hump is due to the second helium ionization zone at a radius of about 0.98 $R_\odot$ while the other one, at a radius of about 0.99 $R_\odot$, is located inside the H I and He I ionization zones. From this figure it is clear that for the model under consideration $0.72 < X < 0.74$. In this case, since all models use the same physics, it is straightforward to estimate the value of X in the new model using the functions $H_1(w)$ with respect to the sequence of reference models. However, if there is some difference in the equation of state or in the mixing-length formulation used to construct the solar models, then the situation is not clear. Figure 2 shows the functions $H_1(w)$ between the EFF reference models and the solar envelope model M7. It is

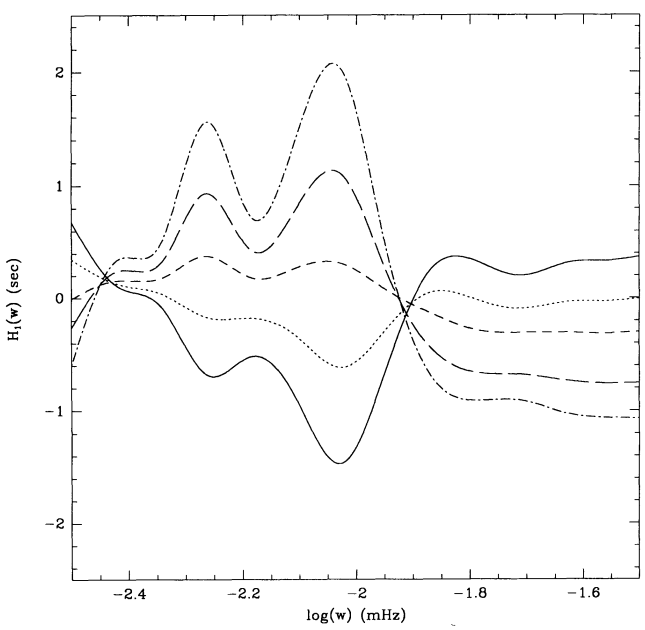

FIG. 1.—Functions $H_1(w)$ between the EFF reference models EFF76 (*solid line*), EFF74 (*dotted line*), EFF72 (*short dashed line*), EFF70 (*long dashed line*), EFF68 (*dot-dashed line*), and the model M1.

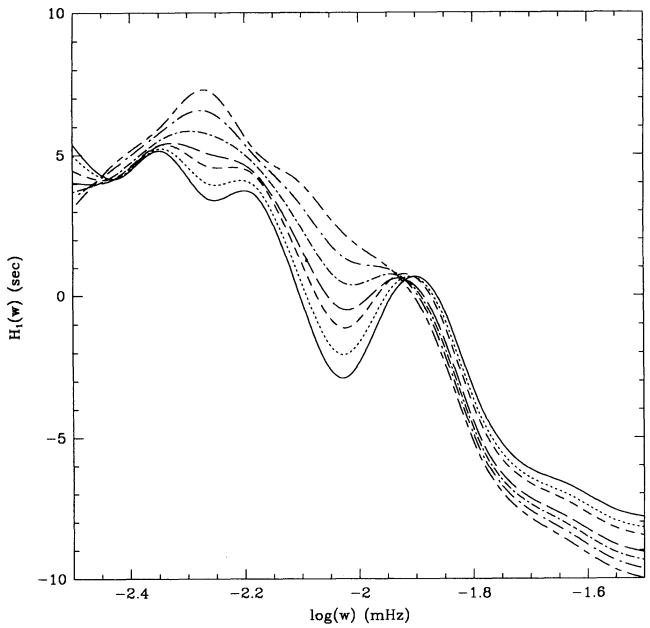

FIG. 2.—Functions $H_1(w)$ between the EFF reference models EFF76 (*solid line*), EFF74 (*dotted line*), EFF72 (*short dashed line*), EFF70 (*long dashed line*), EFF68 (*dot–short dashed line*), EFF66 (*dot–long dashed line*), EFF64 (*short dash–long dashed line*), and the model M7.

clearly difficult to estimate the helium abundance in this model from these curves because of rather steep variation of $H_1(w)$ with w which is superposed on the humps due to helium abundance. From the first hump around log $w \approx -2.1$ mHz it appears that X is between 0.66 and 0.64 in model M7, while the second hump appears to yield a value between 0.68 and 0.72. This problem arises because the He II ionization zone shifts slightly outward when MHD equation of state is used instead of EFF equation of state (Fig. 3). As a result, the difference in sound speed between the models is dominated by the shift in the position of the ionization zone, rather than by the helium abundance. The H I and He I ionization zone does not shift significantly because of the equation of state, since all models start with the same temperature at the photosphere. Thus the signature in this zone may be more useful in measuring helium abundance. However, this zone happens to be very close to the surface where there are considerable uncertainties in the solar models. Furthermore, it is difficult to unambiguously separate the steep trend in $H_1(w)$ using only a narrow range of w.

In order to provide a quantitative measure of helium abundance we use the function $H_1(w)$ between two successive reference models for calibration. For example, if $\phi_{70,72}(w)$ represents the function $H_1(w)$ between models EFF70 and EFF72, then the function $H_1(w)$ between one of the reference models and a test model can be written as

$$H_1(w) = \beta\phi_{70,72}(w) + H_s(w)\,, \qquad (6)$$

where β is a constant and $H_s(w)$ is some smooth function of w which accounts for the differences in the equation of state and the surface layers between the two models. The first term in the above expansion arises from the difference in helium abundance, and the value of β can be calibrated to measure Y. In order to estimate the value of β we can again perform a least-squares fit to the function $H_1(w)$ by expanding the smooth part $H_s(w)$ as a polynomial in log w or in terms of B-spline basis functions in log w. For this purpose it is enough to use a spline with less than 10 knots or a polynomial of degree < 10. Figure 4 shows the result of one such fit.

Having determined the constant β in equation (6), there are two alternatives. One possibility is to keep the reference model in $H_1(w)$ fixed and calibrate the value of β for the difference in helium abundance. If the amplitude of the hump varies linearly with Y, then the difference in Y between the two models should

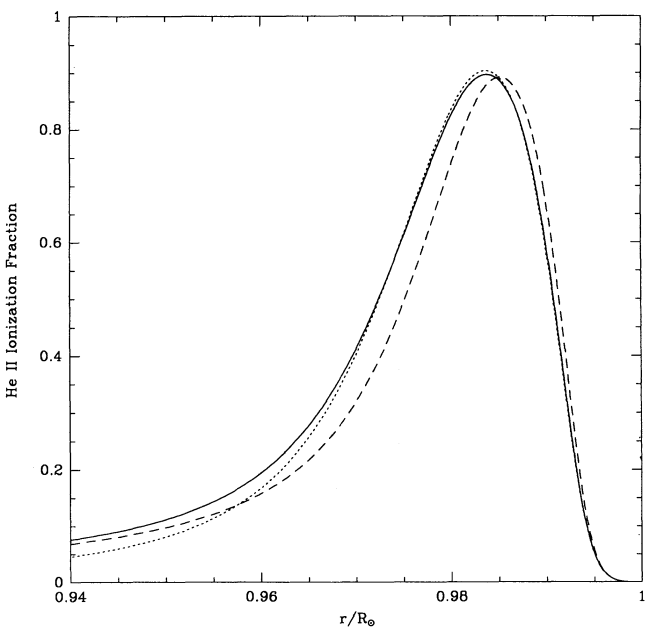

FIG. 3.—He II ionization fraction ($n_{\rm He\,II}/n_{\rm He}$) for the envelope models EFF72 (*solid line*), PLPF72 (*dotted line*), and MHD72 (*dashed line*).

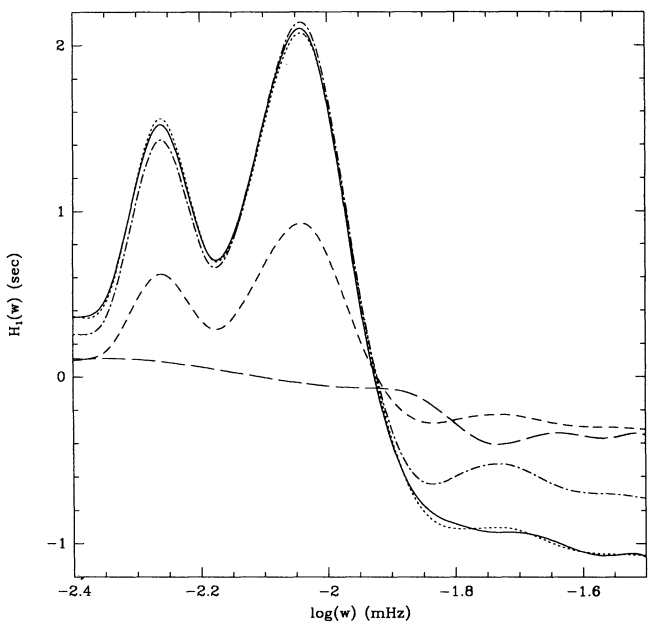

FIG. 4.—The least-squares fit to the function $H_1(w)$ between the reference model EFF68 and model M1, using the calibration curve $\phi_{68,70}(w)$ for determining Y. The dotted line shows the function $H_1(w)$ as obtained from the frequency difference between models EFF68 and M1, the solid line shows the fitted curve, the long dashed line shows the smooth component $H_s(w)$, the dot-dashed line shows $\beta\phi_{68,70}$, and the short dashed line shows the calibration curve $\phi_{68,70}$, which is the function $H_1(w)$ between models EFF68 and EFF70.

be given by 0.02β. Another possibility is to vary the reference model and calculate β as a function of Y in the reference model. The value of Y at which $\beta(Y) = 0$ will give the helium abundance in the test model (or the Sun). In this work we have adopted the second approach, where the equation $\beta(Y) = 0$ is solved by using a least-squares fit to a linear function. As mentioned in § 2, the function $H_1(w)$ is arbitrary to the extent of an additive constant. This constant does not affect the result since it gets absorbed in the smooth part $H_s(w)$.

Figure 5 shows β as a function of Y for the solar envelope model M1, using EFF models for calibration. The four different curves in the figure denote the results obtained using $\phi_{68,70}$, $\phi_{70,72}$, $\phi_{72,74}$, and $\phi_{74,76}$ as the calibration curves. It is clear that the result is not very sensitive to the calibration curve used. The resulting value of Y for this model is 0.2509, 0.2511, 0.2516, and 0.2518 using $\phi_{68,70}$, $\phi_{70,72}$, $\phi_{72,74}$, and $\phi_{74,76}$, respectively, for calibration. This gives an average value of $Y = 0.2514 \pm 0.0004$, which is close to the actual value of Y used in the model. The spread in Y resulting from use of different calibration curves gives an estimate of errors due to uncertainties in the fitting process and other uncertainties in the technique, e.g., the amplitude of the calibration curve may not be a linear function of Y. Other systematic errors, e.g., those due to difference in depths of the He II ionization zone, may also contribute to this error, but the standard deviation will not give any reliable estimate for such errors. These errors can be estimated only by comparing the computed values for test models against the known correct value. It may be noted that the significance of standard deviation using only four to five calibration curves is questionable and can be improved as explained below.

In order to estimate the influence of errors in observed frequency on measurement of Y, we use simulated sets of frequencies where random errors with standard deviation quoted by the observers are added to the calculated model frequencies. For each set of simulated frequencies, we repeat the whole process to estimate the helium abundance Y using each of the four calibration curves. From the distribution of these calculated values of Y we can estimate the expected standard deviation in the results. This error estimate also includes the contribution due to uncertainties in the fitting process considered in the previous paragraph. However, it does not include systematic errors due to differences in the equation of state and other differences arising from surface layers. The systematic errors from uncertainties in the equation of state can be estimated by using test models constructed with one equation of state and finding the helium abundances by employing reference models constructed using a different equation of state.

Using this procedure the estimated value of $Y = 0.2501 \pm 0.0054$ for the model M1 (using EFF reference models), while that for model M7 is 0.3195 ± 0.0061. Thus it can be seen that the estimated error is only marginally larger for model M7, which is constructed using the MHD equation of state, while the actual error in the computed value of Y for the model M7 is much larger.

4. HELIUM ABUNDANCE USING $H_2(\omega)$

Apart from $H_1(w)$ it is also possible to use the function $H_2(\omega)$ to estimate the helium abundance. The procedure is exactly the same as that outlined for $H_1(w)$ in the previous section. We have noted earlier that the function $H_2(\omega)$ is expected to reflect the differences in surface layers of the two models and as such it is possible that the signature of helium abundance may be contaminated by those due to the differences in the surface layers. Figure 6 shows $H_2(\omega)$ for model M1, using models EFF68, EFF70, EFF72, EFF74, and EFF76 as reference models. Once again it is clear that the helium abundance in the model M1 can be easily inferred from these curves. Following the procedure outlined in the previous section we get

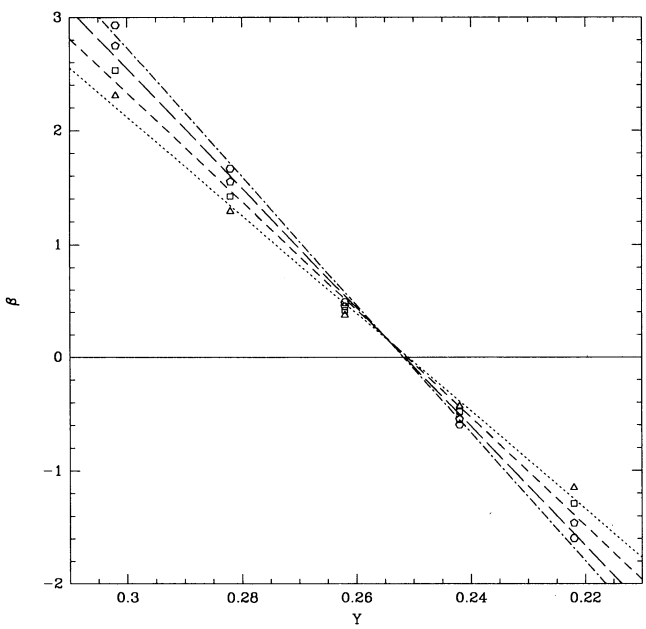

FIG. 5.—β as a function of Y for model M1 with EFF reference models using various calibration curves. The dotted line represents the straight line fit for $\phi_{68,70}$, short dashed line for $\phi_{70,72}$, long dashed line for $\phi_{72,74}$, and dot-dashed line for $\phi_{74,76}$. The actual points are marked by triangles, squares, pentagons, and hexagons for $\phi_{68,70}$, $\phi_{70,72}$, $\phi_{72,74}$, and $\phi_{74,76}$, respectively.

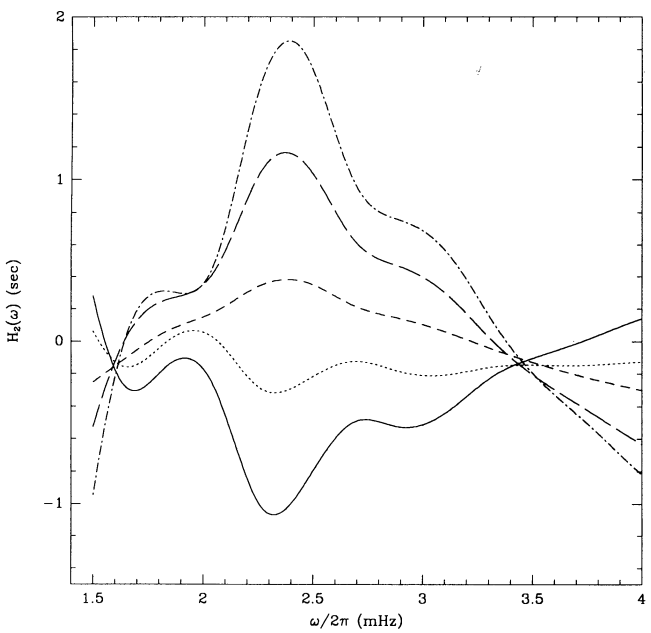

FIG. 6.—Functions $H_2(\omega)$ between the EFF reference models EFF76 (*solid line*), EFF74 (*dotted line*), EFF72 (*short dashed line*), EFF70 (*long dashed line*), EFF68 (*dot-dashed line*), and the model M1.

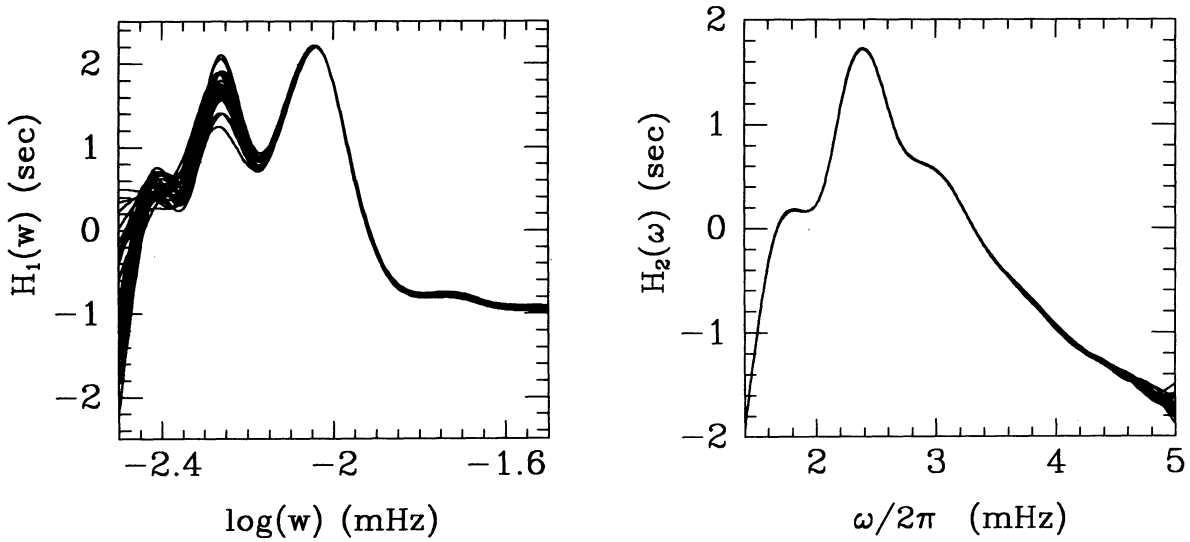

FIG. 7.—Functions $H_1(w)$ and $H_2(\omega)$ between the reference model EFF72 and model M1. The 25 curves represent the functions for 25 sets of simulated frequencies of model M1 after adding random errors according to the quoted variance. The curves have been shifted to account for an arbitrary additive constant.

$Y = 0.2543, 0.2549, 0.2559, 0.2566$ using $\phi_{68,70}$, $\phi_{70,72}$, $\phi_{72,74}$, and $\phi_{74,76}$, respectively as calibration curves. From these four values we get $Y = 0.2554 \pm 0.0010$. The variance gives an estimate of errors due to uncertainties in the fitting procedure. This error estimate is well below the actual error in estimating Y. Thus even when the models are constructed using the same equation of state, there is some systematic error in this technique. However, this systematic error is still much less than the uncertainties introduced because of the variation in the equation of state.

As in the previous section, we can estimate the error due to uncertainties in observed frequencies by using a set of simulated frequencies. Interestingly it turns out that the function $H_2(\omega)$ is remarkably insensitive to the random errors in frequencies. Figure 7 shows the functions $H_1(w)$ and $H_2(\omega)$ between models M1 and EFF72 for a set of 25 simulations. The actual functions $H_1(w)$ and $H_2(\omega)$ calculated by the program are different, because of the uncertainty of an additive constant. The curves shown in the figure are obtained by adding suitable constants to each of the curves to make them agree at $\log w = -2$ mHz for $H_1(w)$ and at $\omega = 2.5$ mHz for $H_2(\omega)$. It is clear that $H_1(w)$ is far more sensitive to the random errors in the frequencies. However, apart from the errors in frequencies there is a substantial systematic error due to differences in the structure of the surface layer which affects $H_2(\omega)$ much more than $H_1(w)$. Thus even though the random error due to uncertainties in the frequencies is much smaller for $H_2(\omega)$, the computed value of Y is not very close to the actual value. Using $H_2(\omega)$, the random errors in Y due to uncertainties in the observed frequencies is only of the order of 10^{-4} in the value computed using one calibration curve. However, using the spread in values due to different calibration curves, we get a somewhat larger variance of 0.0009 in Y.

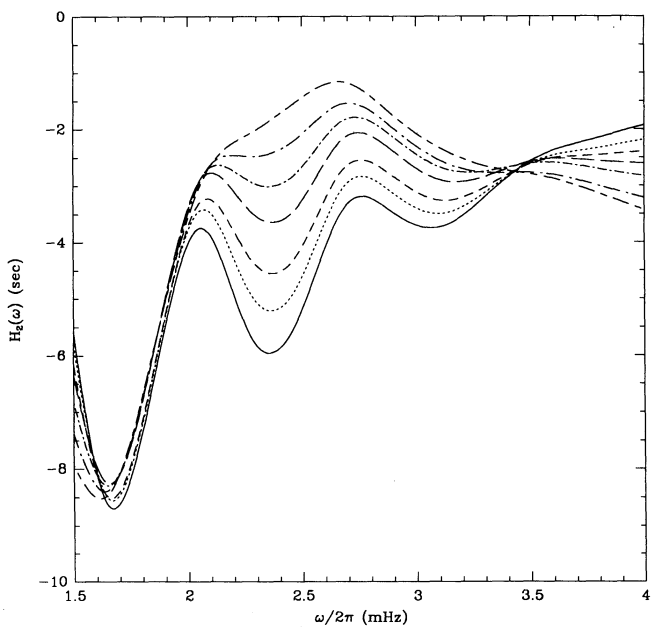

FIG. 8.—Functions $H_2(\omega)$ between the EFF reference models EFF76 (*solid line*), EFF74 (*dotted line*), EFF72 (*short dashed line*), EFF70 (*long dashed line*), EFF68 (*dot–short dashed line*), EFF66 (*dot–long dashed line*), EFF64 (*short dash–long dashed line*), and the model M7.

The estimate of helium abundance using $H_2(\omega)$ is also sensitive to the equation of state. Figure 8 shows $H_2(\omega)$ between the EFF reference models and the model M7, which is based on the MHD equation of state. It is difficult to estimate the helium abundance in model M7 from this figure, and the value estimated from the procedure outlined above turns out to be 0.354 ± 0.006, which is far from the true value for this model.

5. HELIUM ABUNDANCE USING W

We now compute the function W defined by equation (1); for this we need to complete the process of asymptotic inversion for calculating $(c_0 - c)/c_0$ and hence c. Because of numerical errors introduced while taking the derivative of c^2, the computed profile for W is not always smooth, particularly when there is a considerable difference between the two models. In order to overcome this problem we smooth the computed value of c by using a parabolic least-squares fit to the nearest five points (cf. Antia 1991, 463). It turns out that the height of the He II hump in $W(r)$ depends on the choice of the

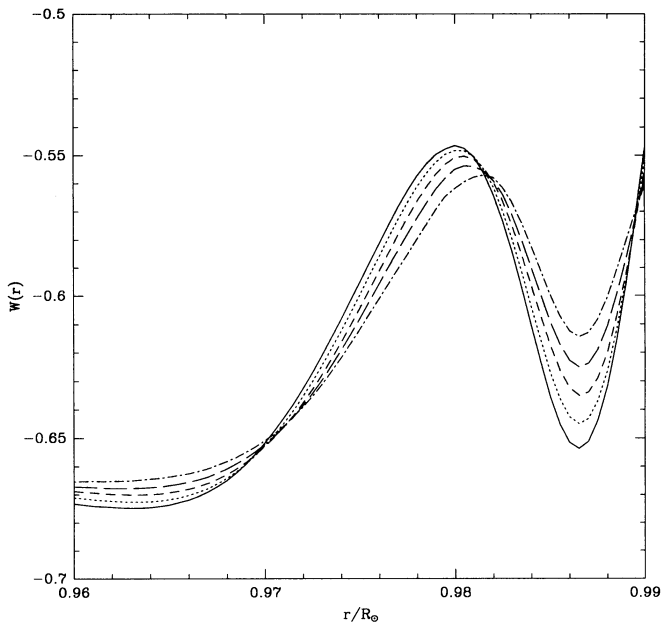

FIG. 9.—Function $W(r)$ for the model M1 obtained by using the EFF reference models EFF76 (*solid line*), EFF74 (*dotted line*), EFF72 (*short dashed line*), EFF70 (*long dashed line*), and EFF68 (*dot-dashed line*).

reference model. Figure 9 displays the function W obtained for the model M1, using EFF68, EFF70, EFF72, EFF74, and EFF76 as reference models. Thus it is clear that it is not possible to provide an absolute calibration using this technique. Figure 10 shows $W(r)$ for models EFF68, EFF70, EFF72, EFF74, EFF76, and the model M1, using the model EFF72 as the reference model. It may be noted that in this case the curve for EFF72 is actually the one obtained using the exact sound speed profile, while for other models it is the one obtained from the sound speed profile given by inversion. It is clear that the height of the He II hump increases systematically with increasing Y, and it is possible to use the heights for the reference models to provide a calibration for Y as a function of height of the hump. Using this calibration we find $Y = 0.2543$ for model M1. This calibration will obviously depend on the reference model used, but it turns out that the final result is not sensitive to the choice of the reference model. Thus using EFF68, EFF70, EFF72, EFF74, and EFF76 as reference models we get $Y = 0.2530$, 0.2539, 0.2543, 0.2541, 0.2548, respectively, for model M1. As explained in § 3, the variance in these estimates give an estimate of errors due to uncertainties in calibration.

To estimate the influence of the errors in frequency on this technique we again use the set of simulated frequencies to compute W for the model under consideration. Using the calibration from a set of reference models we compute Y for each set of simulated frequencies. Using 25 simulations we find $Y = 0.2537 \pm 0.0012$ for model M1, which is in reasonable agreement with the actual value. The systematic errors in this technique also arise from the different depths of the He II humps in models due to differences in the depth of the convection zone or in the equation of state, or in the structure of the outer layers. In fact even when the exact sound speed profile in reference models is used to compute $W(r)$, the height of the He II hump depends on the equation of state (Fig. 11). It may be noted that $W(r)$ for MHD models is not very smooth, probably owing to interpolation within the equation of state tables.

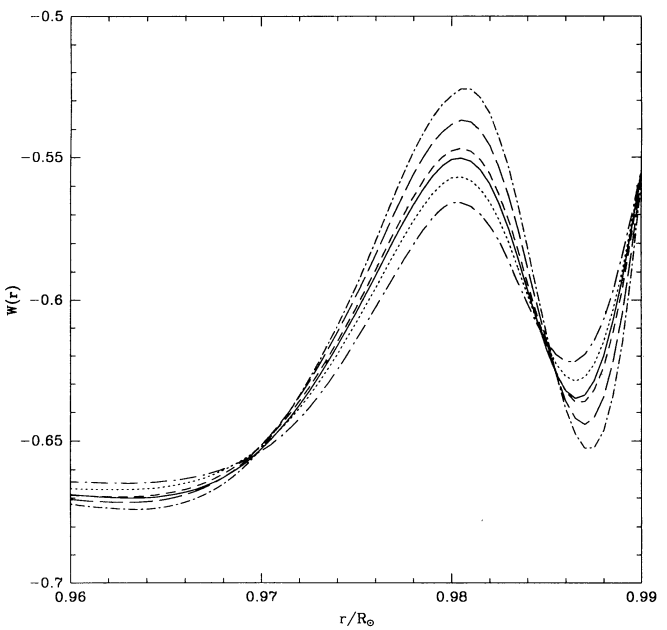

FIG. 10.—Function $W(r)$ for the test model M1 and the EFF reference models obtained by using EFF72 as the reference model. The solid line represents $W(r)$ for model M1; dot–long dashed line, for EFF76; dotted line, for EFF74; short dashed line, for EFF72; long dashed line, for EFF70; and dot–short dashed line, for EFF68.

6. RESULTS

We have used all three techniques described in the previous sections to estimate the helium abundance in the test models and in the Sun using different reference models. For the Sun we adopt the observed frequencies of Libbrecht et al. (1990). The results are summarized in Table 2, which gives the calculated value of the helium abundance in percentage. The errors

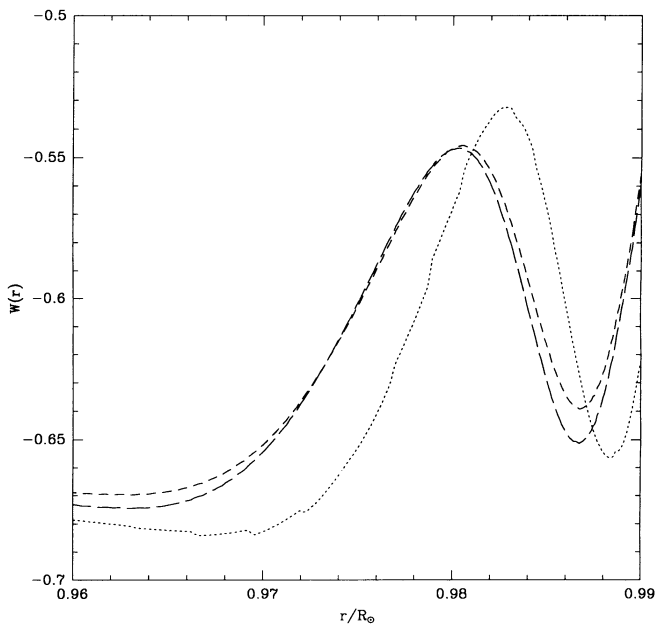

FIG. 11.—Function $W(r)$ for reference models EFF72 (*short dashed line*), PLPF72 (*long dashed line*), and MHD72 (*dotted line*) using the exact sound speed in the respective models.

TABLE 2

DETERMINING Y FOR TEST MODELS

			EFF REFERENCE MODELS			PLPF REFERENCE MODELS			MHD REFERENCE MODELS		
MODEL	EOS	Y_{exact}	$H_1(w)$	$H_2(\omega)$	$W(r)$	$H_1(w)$	$H_2(\omega)$	$W(r)$	$H_1(w)$	$H_2(\omega)$	$W(r)$
M1	EFF	25.00	25.01 ± 0.54	25.54 ± 0.09	25.37 ± 0.12	25.66 ± 0.57	26.22 ± 0.11	27.02 ± 0.17	20.26 ± 0.31	16.51 ± 0.37	21.21 ± 1.10
M2	EFF	26.22	25.62 ± 0.53	28.22 ± 0.19	27.45 ± 0.14	26.25 ± 0.55	28.83 ± 0.03	29.06 ± 0.11	20.61 ± 0.30	17.85 ± 0.03	22.40 ± 0.52
M3	EFF	31.45	36.39 ± 0.82	41.87 ± 0.86	42.14 ± 0.39	36.39 ± 1.09	41.37 ± 1.30	42.99 ± 0.46	31.60 ± 0.29	33.00 ± 0.28	35.57 ± 0.17
M4	EFF	26.00	26.20 ± 0.55	26.36 ± 0.06	26.12 ± 0.11	26.82 ± 0.58	27.01 ± 0.16	27.72 ± 0.19	20.99 ± 0.31	17.08 ± 0.29	21.73 ± 0.99
M5	PLPF	26.93	25.75 ± 0.57	26.44 ± 0.26	24.84 ± 0.20	26.41 ± 0.56	27.13 ± 0.05	26.55 ± 0.10	20.45 ± 0.32	16.44 ± 0.18	20.88 ± 1.02
M6	PLPF	23.82	22.95 ± 0.56	23.45 ± 0.18	21.82 ± 0.15	23.63 ± 0.56	24.23 ± 0.03	23.60 ± 0.09	18.66 ± 0.33	14.86 ± 0.56	19.30 ± 1.53
M7	MHD	27.00	31.95 ± 0.61	35.39 ± 0.63	33.74 ± 0.13	32.25 ± 0.77	35.36 ± 0.95	35.02 ± 0.11	26.75 ± 0.29	26.91 ± 0.07	26.96 ± 0.11
Sun	...	...	30.85 ± 0.60	32.34 ± 0.59	30.55 ± 0.21	31.22 ± 0.74	32.50 ± 0.85	31.98 ± 0.13	25.20 ± 0.31	24.12 ± 0.11	24.04 ± 0.41

quoted in this table are the standard deviation in the results obtained using 25 sets of simulated frequencies. This error estimate represents the uncertainty due to errors in the observed frequencies as well as those due to uncertainties in calibration and fitting procedure.

The model M1 is constructed using the EFF equation of state, and we find that the EFF reference models give a reasonably good estimate for the helium abundance. Even so the estimates of Y obtained using $H_2(\omega)$ and $W(r)$ are somewhat different from the true value. This difference could be attributed to the difference in metal abundance in this model and the reference EFF models. The model M2 has the same metal abundance as the reference models, but has a shallower convection zone. As a result we find that the estimated value of Y is somewhat different from the true value. In this case also $H_1(w)$ gives the best result. The model M3 has a very shallow convection zone and in that case the estimated values of Y are quite far from the true value. Thus it appears that $H_2(\omega)$ and $W(r)$ are more sensitive to changes in surface layers. The model M4 has the same depth of convection zone as the reference models, but has a different metal abundance Z as well as different relative abundance of metals. The difference between the true and calculated value of Y for this model should give an estimate of the errors introduced due to difference in metal abundance.

We have constructed models M5 and M6 with the PLPF equation of state to find that the use of the EFF reference models tend to underestimate the value of Y. Using PLPF reference models we get a reasonably good estimate even though these models have been constructed adopting a different form of mixing-length theory and as such have a somewhat different structure for the surface layers. For model M7 which is constructed using the MHD equation of state, the EFF and PLPF reference models give significantly higher estimates for Y. In this case the MHD reference models give a reasonably accurate estimate. It should be noted that this is the only test model which has the same depth of the convection zone as well as the metal abundance as the reference models. In this case all the three techniques give Y within approximately one standard deviation of the true value. Further, $H_2(\omega)$ and $W(r)$ appear to give a slightly better estimate of Y than $H_1(w)$.

It is quite clear from this table that if the test model and the reference models are constructed using the same equation of state and if the convection zone depths are not very different, then the helium abundance can be determined very reliably. The thickness of the convection zone in some sense determines the depth of the He II ionization zone, since both these depths are essentially controlled by the structure of the surface layers, below which the temperature gradient is practically adiabatic. The sensitivity of Y to the depth of the convection zone is not a very serious issue, since the depth is known fairly accurately (Christensen-Dalsgaard et al. 1991) from helioseismic data.

In almost all cases where the test model has the same equation of state as the reference models, the first technique using $H_1(w)$ appears to give better results. The other methods appear to be more sensitive to changes in the surface layers. Thus for model M2 which has a somewhat different depth of convection zone $H_2(\omega)$ and $W(r)$ yield results which are quite far from the correct value. The function $H_2(\omega)$ is expected to be more sensitive to changes in surface layers, since it is supposed to reflect the uncertainties in these layers. On the other hand, the function $W(r)$ is essentially determined by $H_1(w)$ and is not expected to be any more sensitive to surface layers than $H_1(w)$. However, calculating $W(r)$ from $H_1(w)$ requires two numerical differentiations, first while calculating $(c_0 - c)/c_0$ and second while evaluating $W(r)$ using the computed sound speed. These differentiations are likely to enhance the errors thus making it more difficult to separate out the signal.

It is clear from Table 2 that in those cases where the reference models and the test model use different equations of state the estimated value of Y is significantly different from the true value. The discrepancy is particularly significant between MHD and EFF and between MHD and PLPF equations of state. As mentioned in § 3, this error arises from a shift in the depth of the He II ionization zone. Because of this shift there is a steep variation in $H_1(w)$ as seen in Figure 2. The steep gradient in $H_1(w)$ interferes with the hump in the calibration curve, and it is not possible to isolate the smooth part $H_s(w)$ and the calibration part in equation (6). As a result the computed value of Y obtained using the procedures outlined in §§ 3–5 turns out to be unreliable. The He II hump in Figure 2 appears to give a value of Y between 0.32 and 0.34, which roughly agrees with the value obtained using the procedure outlined earlier but is far from the true value of 0.27 for this model. However, a close look at the figure shows that from the other hump due to H I and He I ionization zone we can infer a value of between 0.26 and 0.30 for Y, which is close to the true value. Thus it appears that the first ionization zone which does not shift appreciably due to variation in equation of state may give a more reliable estimate of Y. Unfortunately it is very difficult to get a reliable quantitative estimate of Y using only a very small part of this curve, since it is not possible to separate the hump from the smooth variation in $H_1(w)$ unambiguously.

It may be noted that the reference models using MHD equation of state cover a limited range of 0.68–0.76 for X, to which our MHD tables are restricted. When we try to use this cali-

bration to determine the helium abundance in models constructed using other equations of state, the resulting value of X may come out to be larger than 0.76, thus requiring some extrapolation of the calibration curves. Because of this extrapolation the MHD reference models give much larger errors for Y in models using EFF or PLPF equation of state.

One source of systematic error in the determination of helium abundance is the difference in metal abundance. The ionization zones of metals may coincide with those of He II thus giving an additional signal due to differences in metal abundances. The metal abundance is known reasonably well in the solar envelope, but because of constraints on computer time, all ionization levels of all metals cannot be incorporated in the equation of state calculations, thus effectively giving rise to differences in metal abundances. In particular, the MHD equation of state uses only C, N, and O in solar abundance and the rest of the metal abundance is filled by Fe. In order to estimate the error due to this difference, we have constructed one solar envelope model (model M4) using this metal abundance. Considering that this model has the same hydrogen abundance as one of the reference models, the only uncertainty in determination of Y (usng EFF reference models) arises from the difference in metal abundances. From Table 2 it can be seen that this difference is ≈ 0.002, which gives an estimate of error introduced due to differences in metal abundance. Further, since the estimated value of Y for model M4 comes out to be larger than the true value, we expect that the value of Y estimated using MHD models as calibration will come out to be about 0.002 larger than the actual value.

We have used all three sets of reference models to estimate the helium abundance in the Sun from the observed frequencies of Libbrecht et al. (1990). Using the first technique based on $H_1(w)$ we get $Y = 0.2520 \pm 0.0031$, 0.3085 ± 0.0060, and 0.3122 ± 0.007, respectively, from calibration models employing the MHD, EFF, and PLPF equations of state. The errors quoted here are those arising from using differences in calibration curves and the uncertainties in the observed frequencies. It is clear that the systematic errors due to variation in equation of state are much larger than the quoted error. Nevertheless, from Figure 12 which shows the function $H_1(w)$ between the EFF models and the Sun, it can be seen that although the hump due to He II ionization appears to indicate a value of Y between 0.30 and 0.34, the other hump due to H I and He I ionization appears to yield a value of Y between 0.26 and 0.30. The latter is reasonably close to the value obtained using the MHD reference models. Thus the value of Y computed using the MHD calibration models appear to be closer to the true value of Y.

We have shown using test models that the determination of helium abundance is rather sensitive to the equation of state. Since we do not know the equation of state for the Sun, the helium abundance in the Sun cannot be determined unambiguously using these techniques. In order to estimate the systematic error in the determination of the solar helium abundance, it is necessary to find out which of the equations of state is closest to reality. A reasonable measure of this can be obtained by considering the function $H_1(w)$ between the Sun and a reference model. Figures 12 and 13 show the function $H_1(w)$ between the Sun and reference models using, respectively, EFF and MHD equations of state. The results using the PLPF reference models are very similar to those using EFF reference models. For all these cases the function $H_1(w)$ increases steeply for $\log w < -2.4$ mHz. This steep variation is

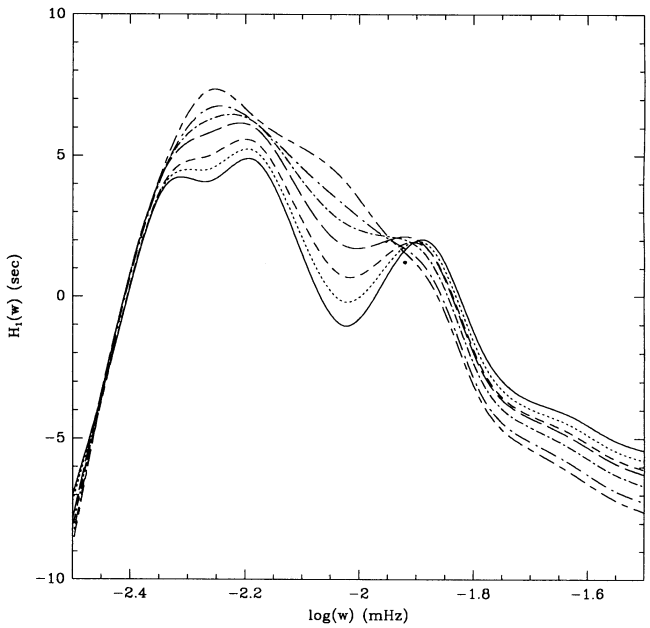

FIG. 12.—Functions $H_1(w)$ between the EFF reference models EFF76 (*solid line*), EFF74 (*dotted line*), EFF72 (*short dashed line*), EFF70 (*long dashed line*), EFF68 (*dot–short dashed line*), EFF66 (*dot–long dashed line*), EFF64 (*short dash–long dashed line*), and the Sun.

most probably due to uncertainties in the surface layers where the stratification is uncertain because of the lack of any reliable theory for stellar convection. Neglecting this part, it is clear that the smooth part of $H_1(w)$ is a slowly increasing function of $\log w$ for the MHD reference models, while for other reference models it decreases rather steeply. The variation in $H_1(w)$ is about a factor of 4 lower using MHD equation of state as compared to that using the EFF equation of state. Thus it is clear that models using MHD equation of state are closer to

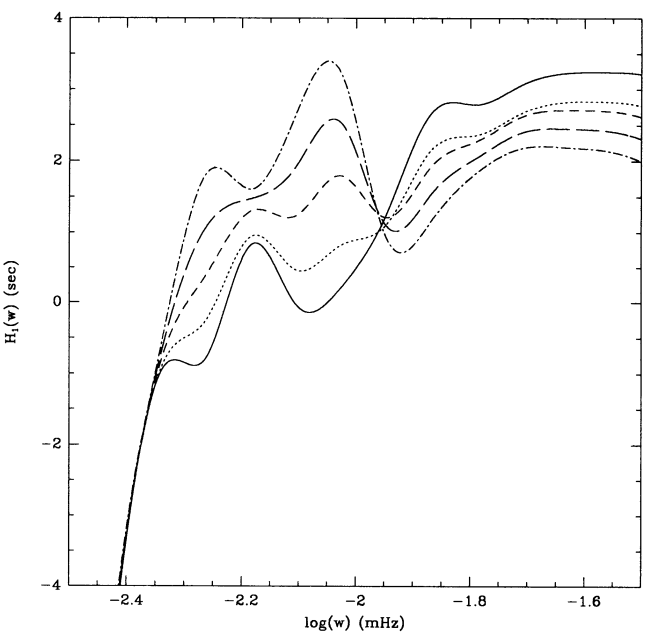

FIG. 13.—Functions $H_1(w)$ between the MHD reference models MHD76 (*solid line*), MHD74 (*dotted line*), MHD72 (*short dashed line*), MHD70 (*long dashed line*), MHD68 (*dot–dashed line*), and the Sun.

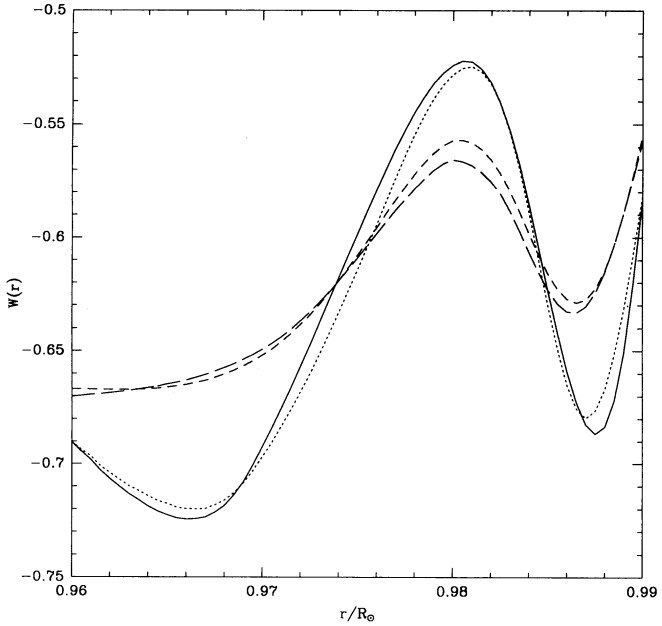

FIG. 14.—Function $W(r)$ for the models EFF74 (*short dashed line*), PLPF7 (*long dashed line*), MHD74 (*dotted line*), and the Sun (*solid line*) using EFF72 as a reference model.

the Sun than those based on other equations of state considered here.

Another indication about which equation of state is closest to that of solar material is provided by $W(r)$. Figure 14 shows the function $W(r)$ for models EFF74, PLPF74, MHD74, and the Sun, obtained using the model EFF72 as the reference model. It is clear that the shape of $W(r)$ for the Sun is closer to that of the MHD model than that for the other models. Thus we expect that the estimated helium abundance using the

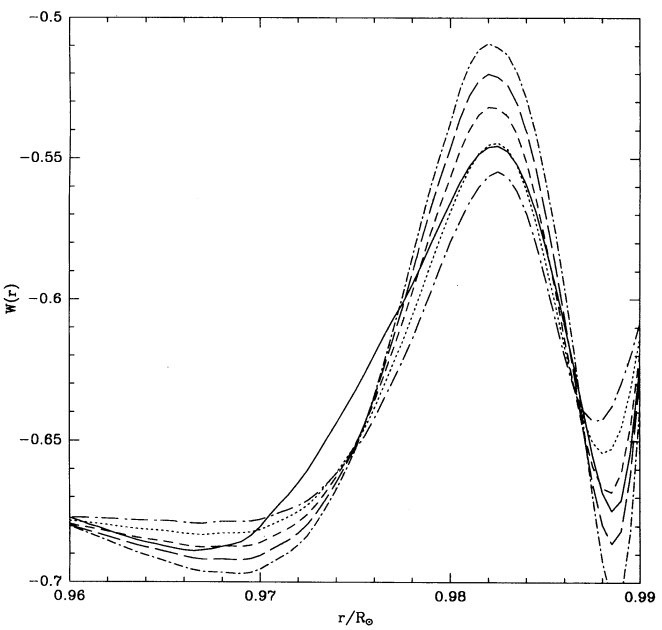

FIG. 15.—Function $W(r)$ for the Sun and the MHD models obtained by using MHD74 as the reference model. The solid line represents $W(r)$ for the Sun; dot–long dashed line, for MHD76; dotted line, for MHD74; short dashed line, for MHD72; long dashed line, for MHD70; and dot–short dashed line, for MHD68.

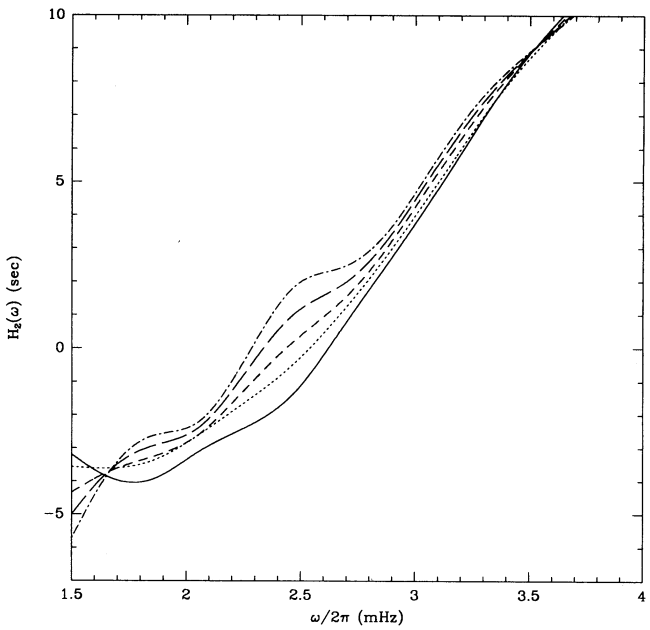

FIG. 16.—Functions $H_2(\omega)$ between the MHD reference models MHD76 (*solid line*), MHD74 (*dotted line*), MHD72 (*short dashed line*), MHD70 (*long dashed line*), MHD68 (*dot-dashed line*), and the Sun.

MHD equation of state is more reliable. Using $W(r)$ with MHD reference models gives $Y = 0.2404 \pm 0.0041$, for the Sun which is somewhat lower than the value obtained using $H_1(w)$. Figure 15 shows the functions $W(r)$ for the MHD reference models and for the Sun, obtained using MHD74 as the reference model. It can be seen that close to the He II hump, the curves for the Sun and MHD74 are very close, thus giving an estimate of $Y \approx 0.24$. However, it is clear from the figure that the two curves differ significantly in regions away from the peak. On the other hand, from Figure 14 where we have used EFF72 as the reference models, it appears that the helium abundance in the Sun is larger than 0.24. Interestingly, in this case the shape of the curves for the Sun and the MHD model is similar. Thus clearly, there are some systematic errors in this technique which are difficult to estimate. In this work we have used the height of the He II hump as a measure of the helium abundance. Instead, if we use the area under the curve to measure the helium abundance, which appears to be more plausible, then the value of Y for the Sun will work out to be higher in accordance with that obtained using $H_1(w)$. In principle it is possible to use the area under the curve rather than the height as a measure of helium abundance, but the problem arises because in all cases it may not be easy to define the boundaries of the hump. Thus it is clear from Figure 15 that depending on where we place the lower limit of the hump, we will get different values of Y. It would be more difficult to estimate the systematic errors in such a calibration.

In order to get an estimate of the error in the calculated value of Y for the Sun using the MHD model we can examine Figures 12 and 13 more carefully. It is clear that the smooth part in $H_1(w)$ has opposite slope for the two equations of state. Hence, we can expect the uncertainty to be of opposite sign in the two cases, which means that the true helium abundance is between the values obtained using these references. Considering the fact that the difference in the estimated helium abundance using the two equations of state is about 0.06, we can

expect that the systematic error in the value obtained using the MHD equation of state may be ≈ 0.015. Apart from this there could be an additional error due to differences in metal abundances, which is estimated to be 0.002. Further, this error is expected to be in the opposite direction, that is the true value of Y may be about 0.002 lower than that estimated using MHD calibration models. It is difficult to pin down the net uncertainty in the estimated value of Y but we may expect it to be ≈ 0.01.

Using $H_2(\omega)$ with MHD reference models yields $Y = 0.2412 \pm 0.0011$, which is somewhat lower than that obtained using $H_1(w)$. The function $H_2(\omega)$ is likely to be affected by the systematic errors arising from differences in the surface layers. Figure 16 shows $H_2(\omega)$ between the MHD reference models and the Sun. It is quite clear from this figure that because of rather steep gradient in the smooth part of $H_2(\omega)$ it is difficult to get a reliable estimate of Y.

7. CONCLUSIONS

We have considered three techniques for estimating the helium abundance in the solar envelope using frequencies of solar oscillations for modes trapped in the convection zone. From tests on known solar models it appears that the function $H_1(w)$ gives a more reliable estimate of Y than either $H_2(\omega)$ or $W(r)$. This technique is not too sensitive to variations in the surface layers either. However, all the techniques are fairly sensitive to the equation of state. Thus, while it is possible to estimate Y fairly well using reference models constructed with the same equation of state, there is a significant systematic error in estimate of Y using different equations of state.

We have used all three sets of reference models to estimate the helium abundance in the Sun from the observed frequencies of Libbrecht et al. (1990). As argued in the previous section the estimate of $Y = 0.252 \pm 0.003$ obtained using the function $H_1(w)$ with the MHD calibration models seems to be more reliable. This value also appears to be supported by the H I and He I hump in $H_1(w)$ between the EFF or PLPF reference models and the Sun.

In order to estimate the systematic error, we can consider the function $H_1(w)$ for the observed frequencies using reference models based on different equations of state. The gradient of smooth part of $H_1(w)$ is about a factor of 4 lower for MHD reference models as compared to EFF or PLPF models, indicating that the MHD equation of state is closer to that of the solar material. Further, this smooth variation in $H_1(w)$ is likely to result in an underestimation of Y, and the actual value could be somewhat higher than the value obtained using the MHD reference models. Apart from variations in the equation of state, there is also some systematic error due to the differences in abundances of heavy elements used in the equation of state calculations. Using test models with different metal abundances we estimate that with the MHD equation of state we are likely to overestimate Y by ≈ 0.002. Thus the two errors are of opposite sign, and it is difficult to estimate the net uncertainty in the computed value of Y, but we may expect it to be less than 0.01.

Our estimate for the helium abundance is consistent with that of Vorontsov et al. (1992) as well as of Christensen-Dalsgaard & Pérez Hernández (1991) and is slightly higher than the value of 0.240 ± 0.005 obtained by Guzik & Cox (1993). Similarly, our estimate is somewhat higher than the value of 0.234 ± 0.006 obtained by Dziembowski et al. (1991) or Kosovichev et al. (1992). It is difficult to pinpoint the source of this discrepancy, but we would like to mention that Kosovichev et al. (1992) have performed all the tests using models constructed with different versions of the same equation of state (MHD), which is likely to underestimate the possible systematic errors due to the difference between the model equations of state and that of the solar material.

We thank W. Däppen for kindly supplying us the tables for the MHD equation of state.

REFERENCES

Antia, H. M. 1991, Numerical Methods for Scientists and Engineers (New Dehli: Tata McGraw-Hill)
Antia, H. M., Chitre, S. M., & Narasimha, D. 1984, ApJ, 282, 574
Christensen-Dalsgaard, J., Däppen, W., & Lebreton, Y. 1988, Nature, 336, 634
Christensen-Dalsgaard, J., Gough, D. O., & Thompson, M. J. 1989, MNRAS, 238, 481
———. 1991, ApJ, 378, 413
Christensen-Dalsgaard, J., & Pérez Hernández, F. 1991, in Challenges to Theories of the Structure of Moderate-Mass Stars, ed. D. O. Gough & J. Toomre (Heidelberg: Springer), 43
Cox, A. N., & Tabor, J. E. 1976, ApJS, 31, 271
Däppen, W., & Gough, D. O. 1986, in Seismology of the Sun and the Distant Stars, ed. D. O. Gough (NATO ASI Ser. C, 169) (Dordrecht: Reidel), 275
Däppen, W., Gough, D. O., Kosovichev, A. G., & Thompson, M. J. 1991, in Challenges to Theories of the Structure of Moderate-Mass Stars, ed. D. O. Gough & J. Toomre (Heidelberg: Springer), 111
Däppen, W., Gough, D. O., & Thompson, M. J. 1988a, in Seismology of the Sun and Sun-like Stars, ed. E. J. Rolfe (ESA SP-286) (Noordwijk: ESA), 505
Däppen, W., Mihalas, D., Hummer, D. G., & Mihalas, B. W. 1988b, ApJ, 332, 261
Dziembowski, W. A., Pamyatnykh, A. A., & Sienkiewicz, R. 1991, MNRAS, 249, 602
Ebeling, W., Kraeft, W. D., & Kremp, D. 1976, Theory of Bound States and Ionization Equilibrium in Plasmas and Solids (Berlin: Akademie Verlag)
Eggleton, P. P., Faulkner, J., & Flannery, B. P. 1973, A&A, 23, 325
Gough, D. O. 1984, Mem. Soc. Astron. Ital., 55, 13
Guzik, J. A., & Cox, A. N. 1993, ApJ, 411, 394
Hummer, D. G., & Mihalas, D. 1988, ApJ, 331, 794
Kosovichev, A. G., Christensen-Dalsgaard, J., Däppen, W., Dziembowski, W. A., Gough, D. O., & Thompson, M. J. 1992, MNRAS, 259, 536
Libbrecht, K. G., Woodard, M. F., & Kaufman, J. M. 1990, ApJS, 74, 1129
Mihalas, D., Däppen, W., & Hummer, D. G. 1988, ApJ, 331, 815
Rogers, F. J. 1977, Phys. Lett., 61A, 358
Rogers, F. J., & Iglesias, C. A. 1992, ApJS, 79, 507
Vernazza, J. E., Avrett, E. H., & Loeser, R. 1973, ApJ, 184, 605
Vorontsov, S. V., Baturin, V. A., & Pamyatnykh, A. A. 1992, MNRAS, 257, 32